Water Resources and Industry 28 (2022) 100183

Contents lists available at ScienceDirect

Water Resources and Industry

journal homepage: www.elsevier.com/locate/wri

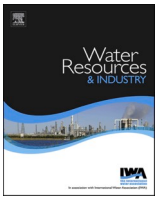

Degradation of 1,4-dioxane by sono-activated persulfates for water and wastewater treatment applications

Shirish Sonawane [a,b,**], Kirill Fedorov [c], Manoj P. Rayaroth [a], Grzegorz Boczkaj [c,d,*]

[a] Gdansk University of Technology, Faculty of Chemistry, Department of Process Engineering and Chemical Technology, G. Narutowicza St. 11/12, 80-233, Gdansk, Poland
[b] National Institute of Technology Warangal, Telangana State, 506004, India
[c] Gdansk University of Technology, Faculty of Civil and Environmental Engineering, Department of Sanitary Engineering, G. Narutowicza St. 11/12, 80-233, Gdansk, Poland
[d] EkoTech Center, Gdansk University of Technology, G. Narutowicza St. 11/12, 80-233, Gdansk, Poland

ARTICLE INFO

Keywords:
Persulfate
Ultrasound
Cavitation
Mineralization
Wastewater treatment
Radicals

ABSTRACT

This paper presents a hybrid advanced oxidation process (AOP) based on sonocavitational activation of persulfate (PS) for degradation of 1,4-dioxane during wastewater treatment. Application of sono-cavitation effectively convert PS to radical species demonstrating synergistic effect by increasing the reaction rate and reducing the required energy for activation. It is economically feasible and deployed alternative to the direct thermal activation method. A single and two-stage injection of PS were compared to eliminate self-scavenging effects related to excess of oxidant in system. A GC-MS analysis was used to determine the degradation products of dioxane and to propose the degradation mechanism. The studies revealed that the degradation was significantly enhanced by the addition of PS at molar ratio of oxidant to pollutant 4 with a two-stage injection. Under optimal conditions at US density of 105 W/cm^2, dioxane with an initial concentration of 100 mg/L was completely degraded in 120 min.

1. Introduction

1,4-dioxane (dioxane) is a one of the emerging micropollutants in wastewater, groundwater, and drinking water due to its widespread use in the production of paint, surface coatings, detergent, cosmetics, cleaning agents, corrosion inhibitors, etc. Dioxane is a human carcinogen classified as a potential carcinogenic compound (B2 class) by the International Agency for Research on Cancer (IARC). The presence of ppm levels of dioxane in water may cause severe health issues [1,2]. Recent water purification method such as reverse osmosis is inefficient to reject dioxane and its derivatives. Some studies reported that activated sludge process, as well as sewage treatment plants, could remove the dioxane with 30–80% efficiency [3,4].

Recently, several attempts have been made to remove dioxane from various water resources using biofiltration method [5], microbial-based degradation [6], advanced oxidation processes (AOPs) [7], including TiO_2/H_2O_2/UV process, H_2O_2/Fe(II) [8,9], metal oxide catalyst [10], solar photolysis with N-doped immobilized photocatalyst [11], Fenton-like catalyst (combination of Fe^0 and

* Corresponding author. Gdansk University of Technology, Faculty of Civil and Environmental Engineering, Department of Sanitary Engineering, 80 – 233, Gdansk, G. Narutowicza St. 11/12, Poland.
** Corresponding author. National Institute of Technology Warangal, Chemical Engineering Department, TS, 506004, India.
E-mail addresses: shirish@nitw.ac.in (S. Sonawane), grzegorz.boczkaj@pg.edu.pl (G. Boczkaj).

https://doi.org/10.1016/j.wri.2022.100183
Received 23 March 2022; Received in revised form 1 June 2022; Accepted 28 June 2022
Available online 30 June 2022

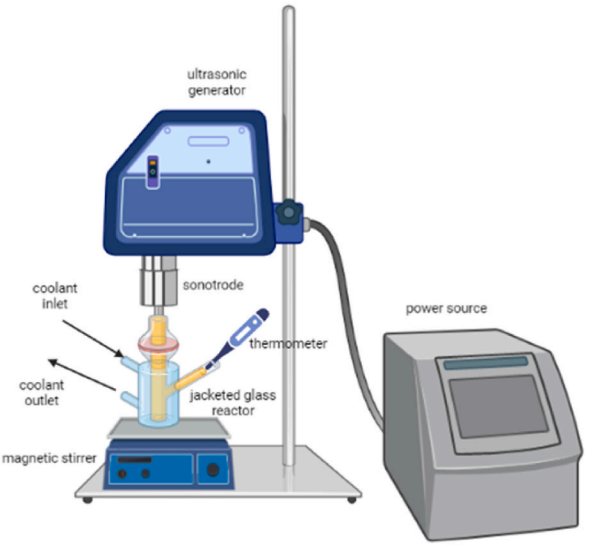

Fig. 1. Experimental setup for the sonochemical degradation.

UV light), electrochemical oxidation [12], ceramic membrane-based removal [13], etc. However, only the partial removal of dioxane was reported in most of the AOPs and therefore it requires the combination of two or more methods. Most of AOPs require high energy input, large catalyst loadings, complex configuration of the reactor system, which prohibit the implementation of these methods on industrial scale.

Application of persulfate (PS) in wastewater treatment is getting increasing attention due to high stability, low cost, and non-selective reaction chemistry paths that can achieve complete mineralization of treated contaminants [14–17]. Compared to H_2O_2, the consumption of PS over the moles of the contaminant was found lower as the reaction stoichiometric efficiency (RSE) of PS is higher [18–21]. Thus, studies on activation of PS using iron powder and Fe-based metal-organic frameworks (MOFs) resulted in RSE of 5 and ~40%, respectively [18–20]. In the case of UV-254 and heat-activated PS, the values of RSE were up to 55 and 60%, respectively [21,22]. As a part of AOPs, PS was highlighted effective in the degradation of chloramphenicol [23], benzoic acid [24]. Heat-activated PS engenders sulfate ($SO_4^{\bullet-}$) and hydroxyl ($HO^{\bullet}$) radicals which are more commanding activator capable to effectively oxidize the organic content in wastewater [25,26]. Heat-activated PS was used in industrial wastewater for removal of dinitrodiazophenol [27], bisphenol [28,29], chloramphenicol [23], carbon tetrachloride [28] lindane [30,31], chloroxylenol [32], mono- and dichlorobenzenes [31,33], etc. Independently, the process based on PS activation has certain limitations derived from the higher activation energy ranging from 140 to 180 kJ/mol. This factor raises the issues which enforce to heat the wastewater (40–80 °C) and introduce large quantity of PS to increase the reaction rate. However, the above issues can be addressed by the use of combination of PS with cavitation-based AOPs. Cavitation is the process which generates a variety of reactive species by generating high local temperature (5000 K) and pressure (6×10^4 kPa) through the collapse of cavitating bubbles [34,35]. The cavitation conditions facilitate mass transport and the generated radicals are responsible for oxidation of pollutants. Some of the successful attempts were reported for degradation of benzene, toluene, ethylbenzene, *o*-xylene (BTEX) mixture using hydrodynamic cavitation and PS [16]. The cavitation can also be combined with catalysts such as zero valent iron, $ZnO/ZnFe_2O_4$, nano size copper, asphaltenes, carbon black in the PS activation to intensify the oxidation processes [36–41].

There are very few reports found on US-assisted dioxane degradation [42], they reported the degradation of dioxane using four different frequencies and reported that US frequencies 358 kHz showed better performance. Son et al. reported the degradation kinetics of dioxane using US with the addition of Fe^0, Fe^{2+} and $S_2O_8^{2-}$ [43], they reported that addition of oxidants not only increased the rate of reaction but also change the kinetic models. The solvents such as ethanol and CCl_4 had a significant effect on the dioxane degradation through the decrease in the thermal effect of cavitation and the generation of reactive chlorine species respectively [44]. In addition, the sono-cavitation processes were effective in the simultaneous degradation of dioxane and trichloroethane degradation [45]. They reported that dioxane and trichloroethane degradation is higher at 15 °C, with PS concertation of 1.50 mmol/L at the frequency of 400 kHz with power 100 W.

Briefly, most of reports shows that PS is being used for degradation of different organic compounds from wastewater with AOPs such as catalyst [39,46], MOFs [20], zero valent metals [18,19,47,48], ozone [49] or hydrodynamic cavitation [16]. Further, there are few reports were found which report the dioxane degradation with US and PS. Therefore, this work was carried out with the following objectives, firstly, to study the effect of US-assisted PS activation in an ultrasonic processor, optimize PS dose comparing single and dual-stage oxidant addition. Next, to study the kinetics of degradation and to identify the intermediate products to propose the degradation pathway.

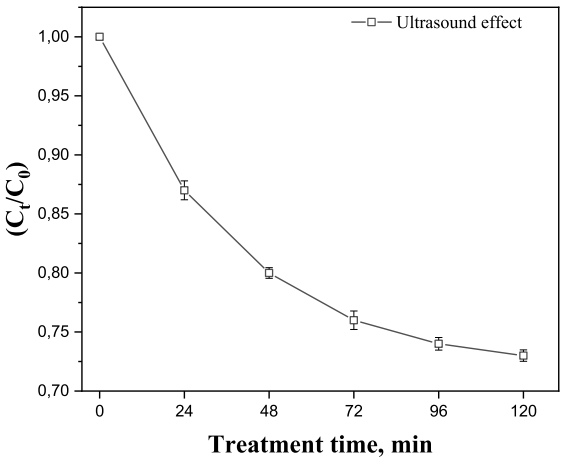

Fig. 2. The sole-cavitation process on the degradation of dioxane; C_0 100 mg/L, Frequency 24 kHz, amplitude = 100%.

2. Materials and methods

2.1. Materials and chemicals

1,4-Dioxane, ($C_4H_8O_2$), sodium persulfate ($Na_2S_2O_8$), dichloromethane, and methanol were purchased from POCH (Poland). *Tert*-butyl alcohol was purchased from Sigma-Aldrich (Germany). All chemicals and solvents were of analytical grade and used without further purification.

2.2. Experimental procedures

Dioxane degradation experiments were performed in ultrasonic probe reactor (Hielscher 400th) (Fig. 1). The degradation was performed at an operating fixed frequency of 24 kHz and sonotrode tip diameter of 22 mm (s24d22D, acoustic power is 180 W). The ultrasound tip active area was 3.8 cm^2, the power output of ultrasound probe was 400 W, hence, 105 W/cm^2 was effective ultrasound intensity for each experiment.

The main variable in the process is amplitude that can be varied from 0 to 100%. In a typical procedure, 500 mL of aqueous solution containing 100 mg/L of dioxane was placed in US steel reactor. The reactor was circulated with cold water supplied from refrigerated bath (Chrompack RTE-110B, Neslab Instruments, USA) to maintain the temperature at 25 ± 2 °C. The details of experimental setup are shown in Fig. 1. PS concentration was varied depending on the ratio between oxidant and dioxane (r_{ox}). Aliquots of samples with an approximate volume of 20 mL were taken before the beginning of treatment, every 20 min in the first hour and each hour within 120 min. All experiments were conducted in deionized water without pH adjustment. pH was measured by Merck non-bleeding pH paper strips.

2.3. Process control by means of gas chromatography

A dispersive liquid-liquid microextraction (DLLME) method was used to preconcentrate the sample of dioxane [50,51]. Briefly, a 10 g of the sample was weighed in a vial and 5 mg of the internal standard (cyclohexanone) was injected into each sample. The mixture is then vigorously shaken. Then 0.5 mL of solvent mixture of dichloromethane and acetone (60:40) was added into the sample. Further, shaking was carried out for 1 min followed by centrifugation (EBA 8S, Hettich, Germany) carried at 5000 rpm for 10 min. A 200 μL of the organic phase was placed into 2 mL vials with 300 μL micro inserts. The vials were sealed with screw-caps equipped with a PTFE-lined silicone septum. The quantitative analysis of dioxane was performed by Clarus 580 (PerkinElmer, USA) gas chromatograph with a flame ionization detector (GC-FID). The GC-FID settings were as follows. Temperature program: 50 °C (5 min) ramped at 10 °C/min to 275 °C (5 min), detector temperature 275 °C A nitrogen was used as carrier gas with volumetric flowrate of 5 mL/min. Detector gases flow rate: air 450 mL/min, hydrogen 40 mL/min. Each sample was tested 2 times with injection volume of 2 μL.

A GCMSQP2010SE (Shimadzu, Japan) was employed for the identification of dioxane degradation by-products. A capillary column (DHA column, 100 m × 0,2 mm ID, 0,1 um) was used to perform GC-MS analysis under following settings. Hydrogen was used as carrier gas (1 mL/min), injection port temperature was 300 °C and GC-MS transfer line temperature was 310 °C. The oven temperature program: was 40 °C (isothermal for 5 min) ramped at 5 °C/min to 220 °C. Ion source (EI, 70 eV) temperature was 200 °C. A mass-to-charge ratio of 34–220 *m/z* was selected for SCAN mode analysis of byproducts.

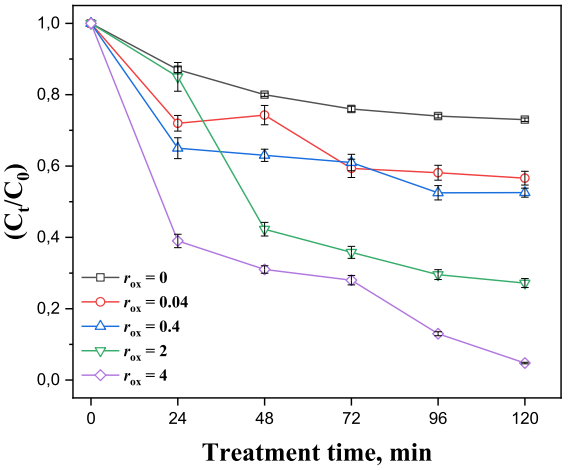

Fig. 3. Effect of addition of PS at different r_{ox} values; C_0 100 mg/L, Frequency 24 kHz, amplitude = 100%.

3. Results and discussion

3.1. Role of ultrasound and oxygen during the degradation

The experiments were performed with 500 mL solution with concentration of 100 ppm of dioxane and taking the samples after each 20 min time. Initially, the experiments were carried out under sole acoustic (sono) cavitation. As can be seen from Fig. 2, less than 25% of dioxane was degraded after 120 min of sonication and no further degradation was observed. Hence, all the batch experiments were carried out for 120 min.

The results indicate that sonocavitation alone is not sufficient to degrade dioxane. The possible reason is that the dioxane is highly hydrophilic. The molecules remain mainly in aqueous phase and do not tend to reach the cavitation bubble region, where the most of radical species are formed during the bubbles collapse. Hence almost 70% of dioxane remains in the solution. The presence of oxygen in the system has also impact on dioxane degradation during sonication [43]. The oxygen has less thermal conductivity, thus, during the bubble collapse the heat is not properly dissipated to the surrounding. Whatever, the degradation is observed, it is because of thermolysis of water to form reactive radicals:

$$H_2O \quad + \ ))) \rightarrow H^{\bullet} + HO^{\bullet} \tag{1}$$

$$H^{\bullet} + O_2 \rightarrow HO_2^{\bullet} \tag{2}$$

$$HO^{\bullet} + HO^{\bullet} \rightarrow H_2O + O^{\bullet} \tag{3}$$

3.2. Effect of persulfate addition on dioxane degradation

Several reports postulated that the addition of PS generates radicals which are giving faster and higher degradation rate compared to sole use of sonocavitation [52–54]. Therefore, an attempt was made to understand the synergistic effect of sonocavitation and PS addition. The molar ratio of oxidant to organic pollutant is defined as r_{ox}:

$$r_{ox} = \frac{moles\ of\ oxidant}{moles\ of\ pollutant} \tag{4}$$

In this study, the degradation of dioxane was evaluated by varying r_{ox} value from 0.04 to 4. Results on optimization of r_{ox} value are provided on Fig. 3. A significant improvement of degradation rate was observed. The highest degradation of 85% was observed at r_{ox} 4. It clearly indicates sonocavitation is effective for PS activation due to high temperature and pressure created during cavitational bubbles collapse which leads to cleavage of the O–O bond in PS molecule (Eq. (5)) [54,55]. There are certain reports which show that PS was effectively activated by US for degradation of organic compounds. For instance, dichloromethane degradation was increased from 20% to 70% comparing sole US and US/PS process [56]. Further, comparing to other AOPs such as ozonation/UV [57], the combination of PS with US leads to complete degradation.

$$S_2O_8^{2-} +))) \rightarrow SO_4^{\bullet -} + SO_4^{2-} + H^+ \tag{5}$$

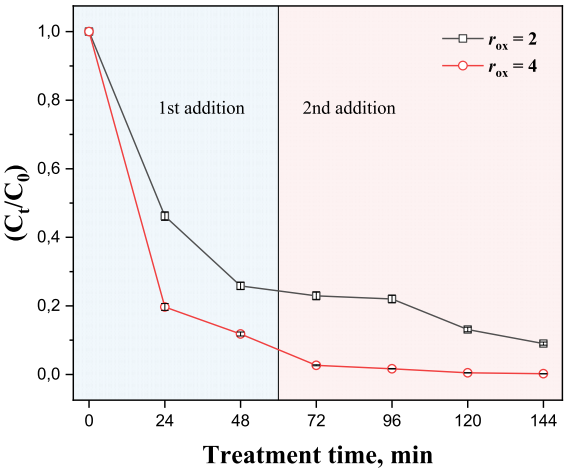

Fig. 4. Effect of two stage addition of PS at different r_{ox}.

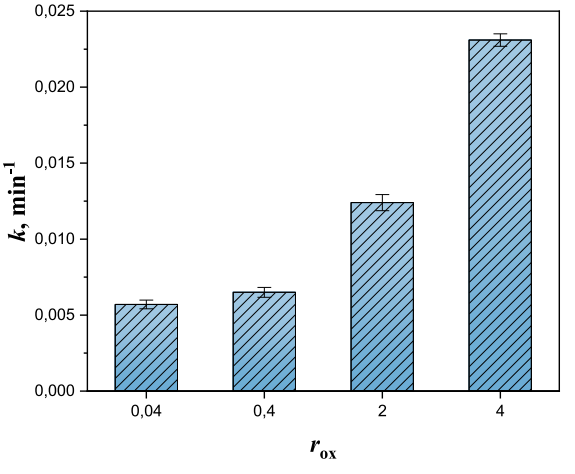

Fig. 5. The effect of r_{ox} on the rate constant, *k*.

3.3. Effect of sequential addition of PS for dioxane degradation

Optimization of oxidant dose mainly relates to concentration of pollutant. However, in every AOP system there is a limiting concentration of oxidants. A self-scavenging effect was observed for most of oxidants, including PS. It follows from reactions of formed radical species with oxidant molecules. In this case, for too high concentrations of oxidant, both radicals and oxidant react together which results in a lack of degradation increase or even decrease of degradation. A reasonable solution to provide high amounts of oxidant without self-scavenging effects seems to be continuous injection of oxidant solution during treatment or sequential injection of defined amounts. In this study a two-stage sequence of oxidant injection was studies. As shown in Fig. 4, the addition of PS was carried out in two stages for the r_{ox} 2 and r_{ox} 4. It was found that with help of the r_{ox} 2, a 90% of degradation was achieved in which 2.5 g/L of PS was added initially and later after 1 h second 2.5 g/L was added. However, still a complete degradation was not achieved, hence, a 5 g/L was added in each stage. As reported in Fig. 3, it was found that direct addition of 5 g/L at initial stage (r_{ox} 2) is not sufficient as only 72% degradation was observed. On the other hand, 10 g/L i.e., two stage addition of 5 g/L (r_{ox} 4) gives the complete degradation of dioxane. Hence, it indicates the optimal dosage of PS required for the effective degradation of dioxane. The r_{ox} 4 – split into two stages showed that even the direct addition does not make difference in the degradation, hence, r_{ox} 4 direct addition at initial stage is preferable and refers to 25% of RSE. The generation of active species such as $SO_4^{\bullet-}$ and $HO^{\bullet}$ radicals from PS requires an activation energy. The energy required for oxidation process is thus significantly lowered under cavitation conditions. The RSE value obtained in this study is in acceptable level compared to the activation of PS using iron powder. However, further profound studies addressing the evolution of PS concentration in PS-based processes in relation with r_{ox} and RSE are required. In addition, comparative studies of PS-based processes in the aspect of economical feasibility using r_{ox}/RSE represent an appealing prospective for future studies.

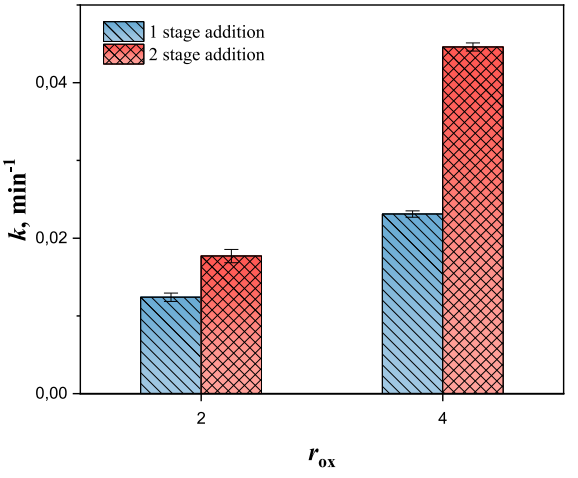

Fig. 6. The k values for the two stage addition of PS at different r_{ox}.

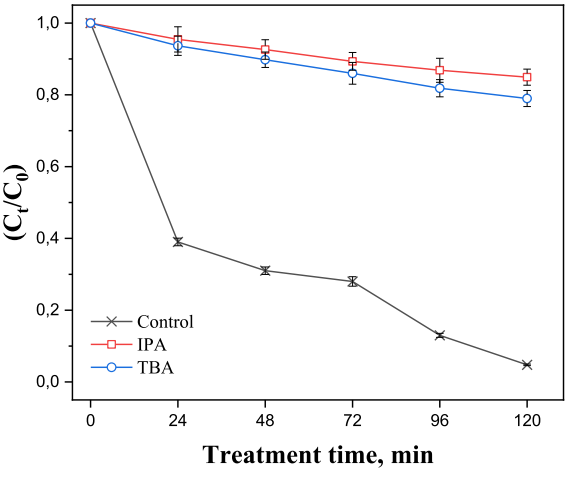

Fig. 7. Effect of radical scavengers on the degradation of dioxane in US/PS at r_{ox} 4.

3.4. Kinetics of dioxane degradation using US and PS addition

The pollutants in AOPs undergo pseudo-first-order kinetics. Degradation rate expression of dioxane can be expressed in terms of the concentration of dioxane and PS using following equation:

$$\frac{-dC_a}{dt} = k\,[C_a]^x[C_{ps}]^y \tag{6}$$

Where, C_a is concentration of dioxane and C_{ps} is concentration of PS, k is reaction rate constant, while x and y represent the order of reaction between dioxane and PS.

However, as the concentration of PS is in excess, the rate will depend on the concentration of the dioxane alone, which is a rate limiting step.

$$\frac{-dC_a}{dt} = k\,[C_a]^x \tag{7}$$

As shown in Fig. 5, the addition of PS showed higher reaction rate constant values from 0.0231, 0.0124, 0.0065, 0.0057 min^{-1} for r_{ox} values of 4, 2, 0.4, 0.04, respectively. As reported in Fig. 6, r_{ox} 4 and 2 with two step addition showed the reaction rate constant value of 0.0446 and 0.0177 min^{-1}, respectively. A comparable reaction rate constant was found in other study on dioxane degradation [45,58]. The results clearly indicate that sonocavitation supports the PS activation for the degradation of dioxane. However, the two stage studies were not performed in the literature, which is possible option to scale up the method for degradation of dioxane.

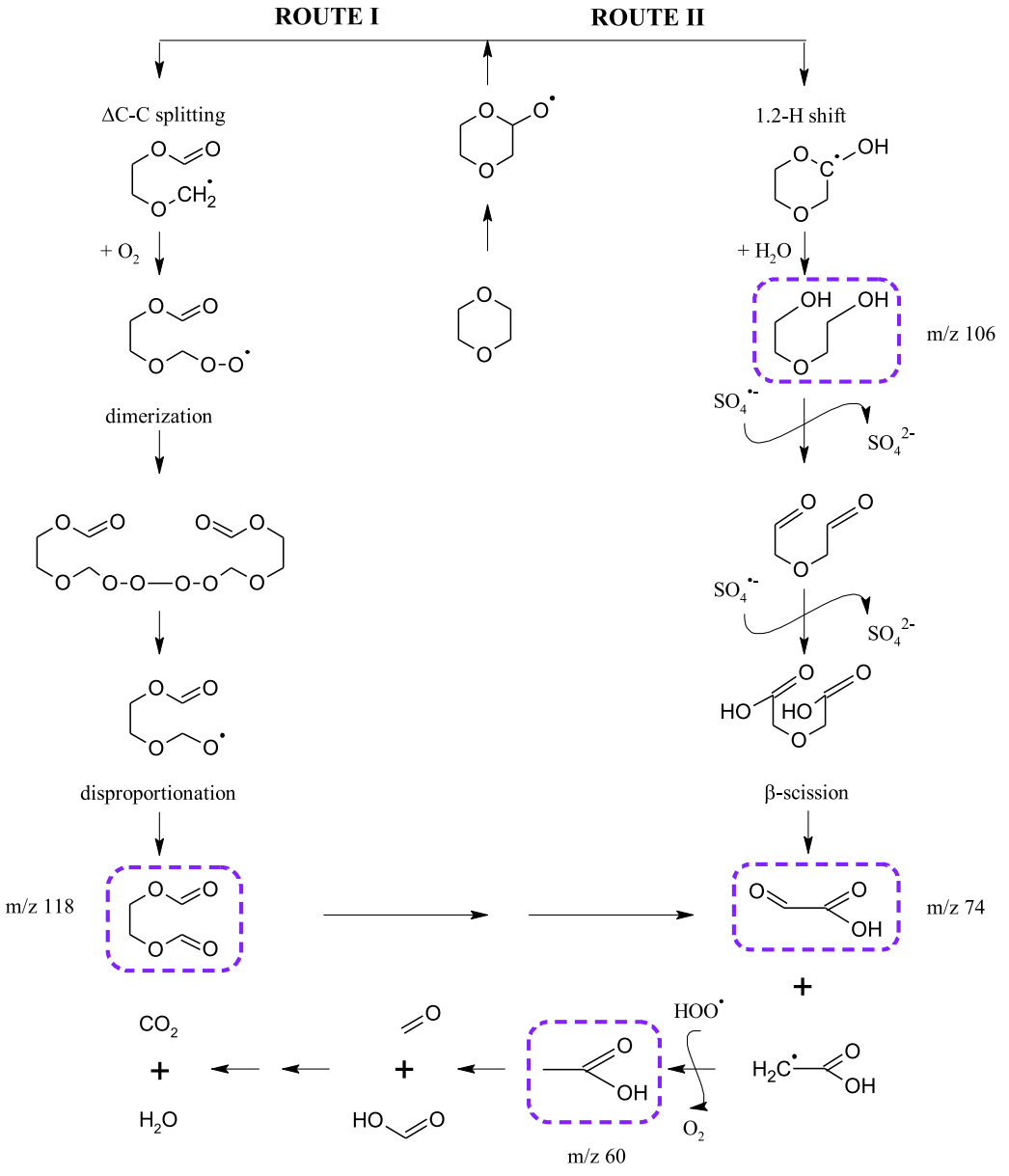

Fig. 8. Proposed reaction pathway of dioxane in US-PS system at r_{ox} 4.

3.5. *Identification of reactive species, intermediate products and the degradation mechanism*

The main reactive species formed in sono-PS are $SO_4^{\bullet-}$ and $HO^{\bullet}$ radicals. Since dioxane is highly hydrophilic the degradation by thermal effect of cavitation can be excluded. Therefore, it is necessary to identify the contribution of each reactive species for the degradation of dioxane in such oxidation process. Scavenging experiment is the most common method in AOPs to identify these species. The alcohols, such as isopropyl alcohol (IPA) and *tert*-butanol (TBA) are the commonly used scavengers for $HO^{\bullet}$ and $SO_4^{\bullet-}$ radicals. Particularly, high reaction rates of IPA with both $HO^{\bullet}$ and $SO_4^{\bullet-}$ radicals (Eqs. (8) and (9)) allow to determine the contribution of both radicals, inhibiting the reaction of dioxane with $SO_4^{\bullet-}$ and $HO^{\bullet}$ radicals. On other hand, the reaction of TBA proceeds faster with $HO^{\bullet}$ radicals and slowly with $SO_4^{\bullet-}$ radicals (Eqs. (10) and (11)), indicating the impact of $SO_4^{\bullet-}$ radicals on the degradation of dioxane [59,60]:

$$IPA + HO^{\bullet} \rightarrow (CH_3)_2C^{\bullet}OH + H_2O \qquad \left(1.9 \times 10^9\ M^{-1}s^{-1}\right) \tag{8}$$

$$IPA + SO_4^{\bullet-} \rightarrow (CH_3)_2C^{\bullet}OH + SO_4^{2-} + H^+ \qquad \left(8.2 \times 10^7\ M^{-1}s^{-1}\right) \tag{9}$$

$$TBA + HO^{\bullet} \rightarrow C^{\bullet}H_2C(CH_3)_2OH + H_2O \qquad \left(6.0 \times 10^{8}\ M^{-1}s^{-1}\right) \tag{10}$$

$$TBA + SO_4^{\bullet -} \rightarrow C^{\bullet}H_2C(CH_3)_2OH + SO_4^{2-} + H^{+} \qquad \left(8.4 \times 10^{5}\ M^{-1}s^{-1}\right) \tag{11}$$

To effectively scavenge radicals, the quenching experiments have been performed with IPA and TBA at a pollutant to scavenger molar ratio of 1:10. The observed results are given in Fig. 7. It can be seen that more than 80% of the initial dioxane content was removed in the sono-cavitation processes. The addition of IPA and TBA reduced the degradation to 15% and 20%, respectively. As IPA is highly reactive with both $HO^{\bullet}$ and $SO_4^{\bullet -}$ radicals, the reduction of dioxane degradation efficiency was significant. TBA selectively quench $HO^{\bullet}$ radicals and the difference in reduction of dioxane degradation efficiency was merely 5%, suggesting the minor contribution of $SO_4^{\bullet -}$ radicals in US/PS process. In other words, these results confirm that $HO^{\bullet}$ radicals are the major reactive species involved in the degradation of dioxane in sono-PS processes (see Fig. 8).

In general, the reaction of $HO^{\bullet}$ radicals with organic contaminants leads to the formation of a number of intermediate products. Therefore, another important step in AOP is the analysis and identification of the possible intermediate products. To examine the degradation pathways, 1000 mg L^{-1} of dioxane solution was treated using US/PS and the transformation products were analyzed using GC-MS in SCAN mode. According to the results, ethylene glycol diformate (EGDF), diethylene glycol, glyoxylic acid and acetic acid were identified as major degradation products in treated samples (Fig. 8). The presence of EGDF and diethylene glycol indicates two possible degradation pathways of dioxane in US-PS process at r_{ox} 4. To our knowledge, diethylene glycol was firstly detected amongst the products of dioxane degradation.

The initial steps of dioxane degradation imply H-abstraction by $HO^{\bullet}$ radicals followed with a series of transformations to form 1,4-dioxan-α-oxyl radical as a primary precursor of intermediates [11,61]. The formation of EGDF (*m/z* 118) refers to the oxidative ring opening mechanism through ΔC-C splitting at the α-C position (Route I). Further fragmentation of EGDF led to the formation of glyoxylic acid (*m/z* 74). This pathway is consistent with previously reported papers [11,45,61,62]. On the other hand, 1,4-dioxan-α-oxyl radical can undergo 1,2-H shift followed by the fission of C–O bond yielding diethylene glycol (*m/z* 106) (Route II). Diethylene glycol is subsequently oxidized and fragmented through β-scission to generate glyoxylic acid and acetic acid (*m/z* 60). It is important to note, that the characteristic peak of EGDF was observed in treated samples within 45 min, suggesting that Route I pathway was predominant during the initial degradation steps. However, EGDF was not found in the samples collected after 60 min and 120 min indicating Route II as predominant. This can be due to the fact that diethylene glycol with α-hydrogen acted as a strong scavenger of $HO^{\bullet}$ radicals, thus, suppressing the concurrent Route I pathway. Finally, these intermediates were not present in effluents after treatment revealing effectiveness of developed AOP.

4. Conclusions

Activation of persulfate under sonocavitation for the degradation of dioxane was studied. Best process obtained for r_{ox} 4 shows the degradation exceeding 95%. Important outcome of this study relates to aspects of sequential addition of oxidant – by two steps to omit risks of self-scavenging between formed radicals and excess of oxidant. Performed comparison revealed an advantageous addition of PS in two stages mode at r_{ox} 4, providing complete degradation of dioxane in 120 min showing 25% of RSE. The degradation kinetics of dioxane followed the first order reaction, and showed the highest *k* value at r_{ox} 4 of 0.0231 min^{-1} and 0.0446 min^{-1} for single and two stage addition of PS respectively. The scavenging experiment and the product analysis clearly showed that the mechanism of dioxane degradation proceeded through $SO_4^{\bullet -}$ and $HO^{\bullet}$ radicals, sonolytic decomposition and oxidation to yield tetraoxide formation converting it into ethylene glycol diformate (EGDF), diethylene glycol, glyoxylic acid and acetic acid.

CRediT authorship contribution statement

Shirish Sonawane: Investigation, Conceptualization, Writing - Original Draft, Validation, Data Curation, Writing - Review & Editing.

Kirill Fedorov: Investigation, Writing - Original Draft, Writing - Review & Editing.

Manoj P. Rayaroth: Investigation, Writing - Original Draft, Writing - Review & Editing.

Grzegorz Boczkaj: Conceptualization, Methodology, Validation, Writing - Original Draft, Writing - Review & Editing, Supervision, Project administration, Funding acquisition.

Declaration of competing interest

The authors declare that they have no known competing financial interests or personal relationships that could have appeared to influence the work reported in this paper.

Acknowledgements

The authors gratefully acknowledge financial support from the National Science Centre, Warsaw, Poland for project OPUS nr UMO-2017/25/B/ST8/01364. Dr Shirish Sonawane acknowledge to the Ulam program of the Polish National Agency for Academic Exchange (NAWA) (Grant number: PPN/ULM/2020/1/00037/U/00001).

References

[1] A. Abe, Distribution of 1,4-dioxane in relation to possible sources in the water environment, Sci. Total Environ. 227 (1999) 41–47, https://doi.org/10.1016/S0048-9697(99)00003-0.

[2] L.A. Schaider, R.A. Rudel, J.M. Ackerman, S.C. Dunagan, J.G. Brody, Pharmaceuticals, perfluorosurfactants, and other organic wastewater compounds in public drinking water wells in a shallow sand and gravel aquifer, Sci. Total Environ. 468–469 (2014) 384–393, https://doi.org/10.1016/J.SCITOTENV.2013.08.067.

[3] D.K. Stepien, P. Diehl, J. Helm, A. Thoms, W. Püttmann, Fate of 1,4-dioxane in the aquatic environment: from sewage to drinking water, Water Res. 48 (2014) 406–419, https://doi.org/10.1016/J.WATRES.2013.09.057.

[4] A. Tanabe, Y. Tsuchida, T. Ibaraki, K. Kawata, Impact of 1, 4-dioxane from domestic effluent on the agano and shinano rivers, Japan, Bull. Environ. Contam. Toxicol. 76 (2006) 44–51.

[5] C.S. Lee, C. Asato, M. Wang, X. Mao, C.J. Gobler, A.K. Venkatesan, Removal of 1,4-dioxane during on-site wastewater treatment using nitrogen removing biofilters, Sci. Total Environ. 771 (2021), 144806, https://doi.org/10.1016/J.SCITOTENV.2020.144806.

[6] M. Li, Y. Liu, Y. He, J. Mathieu, J. Hatton, W. DiGuiseppi, P.J.J. Alvarez, Hindrance of 1,4-dioxane biodegradation in microcosms biostimulated with inducing or non-inducing auxiliary substrates, Water Res. 112 (2017) 217–225, https://doi.org/10.1016/J.WATRES.2017.01.047.

[7] T. Vescovi, H.M. Coleman, R. Amal, The effect of pH on UV-based advanced oxidation technologies – 1,4-Dioxane degradation, J. Hazard Mater. 182 (2010) 75–79, https://doi.org/10.1016/J.JHAZMAT.2010.06.001.

[8] H.M. Coleman, V. Vimonses, G. Leslie, R. Amal, Degradation of 1,4-dioxane in water using TiO2 based photocatalytic and H2O2/UV processes, J. Hazard Mater. 146 (2007) 496–501, https://doi.org/10.1016/J.JHAZMAT.2007.04.049.

[9] P. Ghosh, A.N. Samanta, S. Ray, Oxidation kinetics of degradation of 1,4-dioxane in aqueous solution by H2O2/Fe(II) system, J. Environ. Sci. Heal. Part A. 45 (2010) 395–399, https://doi.org/10.1080/10934520903538954.

[10] K.N. Heck, Y. Wang, G. Wu, F. Wang, A.-L. Tsai, D.T. Adamson, M.S. Wong, Effectiveness of metal oxide catalysts for the degradation of 1,4-dioxane, RSC Adv. 9 (2019) 27042–27049, https://doi.org/10.1039/C9RA05007H.

[11] H. Barndõk, D. Hermosilla, C. Han, D.D. Dionysiou, C. Negro, Á. Blanco, Degradation of 1,4-dioxane from industrial wastewater by solar photocatalysis using immobilized NF-TiO2 composite with monodisperse TiO2 nanoparticles, Appl. Catal. B Environ. 180 (2016) 44–52, https://doi.org/10.1016/J.APCATB.2015.06.015.

[12] J.R. Jasmann, T. Borch, T.C. Sale, J. Blotevogel, Advanced electrochemical oxidation of 1,4-dioxane via dark catalysis by novel titanium dioxide (TiO2) pellets, Environ. Sci. Technol. 50 (2016) 8817–8826, https://doi.org/10.1021/acs.est.6b02183.

[13] G. Scaratti, A. De Noni Júnior, H.J. José, R. de Fatima Peralta Muniz Moreira, 1,4-Dioxane removal from water and membrane fouling elimination using CuO-coated ceramic membrane coupled with ozone, Environ. Sci. Pollut. Res. 27 (2020) 22144–22154, https://doi.org/10.1007/s11356-019-07497-6.

[14] A. Fernandes, P. Makoś, J.A. Khan, G. Boczkaj, Pilot scale degradation study of 16 selected volatile organic compounds by hydroxyl and sulfate radical based advanced oxidation processes, J. Clean. Prod. 208 (2019) 54–64, https://doi.org/10.1016/j.jclepro.2018.10.081.

[15] M.P. Rayaroth, C.T. Aravindakumar, N.S. Shah, G. Boczkaj, Advanced oxidation processes (AOPs) based wastewater treatment - unexpected nitration side reactions - a serious environmental issue: a review, Chem. Eng. J. 430 (2022), 133002, https://doi.org/10.1016/J.CEJ.2021.133002.

[16] K. Fedorov, X. Sun, G. Boczkaj, Combination of hydrodynamic cavitation and SR-AOPs for simultaneous degradation of BTEX in water, Chem. Eng. J. (2020), https://doi.org/10.1016/j.cej.2020.128081.

[17] M. Gągol, E. Cako, K. Fedorov, R.D.C. Soltani, A. Przyjazny, G. Boczkaj, Hydrodynamic cavitation based advanced oxidation processes: studies on specific effects of inorganic acids on the degradation effectiveness of organic pollutants, J. Mol. Liq. 307 (2020), https://doi.org/10.1016/j.molliq.2020.113002.

[18] A. Ghauch, G. Ayoub, S. Naim, Degradation of sulfamethoxazole by persulfate assisted micrometric Fe0 in aqueous solution, Chem. Eng. J. 228 (2013) 1168–1181, https://doi.org/10.1016/J.CEJ.2013.05.045.

[19] G. Ayoub, A. Ghauch, Assessment of bimetallic and trimetallic iron-based systems for persulfate activation: application to sulfamethoxazole degradation, Chem. Eng. J. 256 (2014) 280–292, https://doi.org/10.1016/J.CEJ.2014.07.002.

[20] R. El Asmar, A. Baalbaki, Z. Abou Khalil, S. Naim, A. Bejjani, A. Ghauch, Iron-based metal organic framework MIL-88-A for the degradation of naproxen in water through persulfate activation, Chem. Eng. J. 405 (2021), 126701, https://doi.org/10.1016/J.CEJ.2020.126701.

[21] A. Baalbaki, N. Zein Eddine, S. Jaber, M. Amasha, A. Ghauch, Rapid quantification of persulfate in aqueous systems using a modified HPLC unit, Talanta 178 (2018) 237–245, https://doi.org/10.1016/J.TALANTA.2017.09.036.

[22] S. Al Hakim, S. Jaber, N. Zein Eddine, A. Baalbaki, A. Ghauch, Degradation of theophylline in a UV254/PS system: matrix effect and application to a factory effluent, Chem. Eng. J. 380 (2020), 122478, https://doi.org/10.1016/J.CEJ.2019.122478.

[23] M. Nie, Y. Yang, Z. Zhang, C. Yan, X. Wang, H. Li, W. Dong, Degradation of chloramphenicol by thermally activated persulfate in aqueous solution, Chem. Eng. J. 246 (2014) 373–382, https://doi.org/10.1016/J.CEJ.2014.02.047.

[24] N. Zrinyi, A.L.T. Pham, Oxidation of benzoic acid by heat-activated persulfate: effect of temperature on transformation pathway and product distribution, Water Res. 120 (2017) 43–51, https://doi.org/10.1016/J.WATRES.2017.04.066.

[25] A. Fernandes, P. Makoś, G. Boczkaj, Treatment of bitumen post oxidative effluents by sulfate radicals based advanced oxidation processes (S-AOPs) under alkaline pH conditions, J. Clean. Prod. 195 (2018) 374–384, https://doi.org/10.1016/j.jclepro.2018.05.207.

[26] A.J. Brodowska, A. Nowak, K. Śmigielski, Ozone in the food industry: principles of ozone treatment, mechanisms of action, and applications: an overview, Crit. Rev. Food Sci. Nutr. 58 (2018) 2176–2201, https://doi.org/10.1080/10408398.2017.1308313.

[27] L. Wei, W. Chen, Q. Li, Z. Gu, A. Zhang, Treatment of dinitrodiazophenol industrial wastewater in heat-activated persulfate system, RSC Adv. 8 (2018) 20603–20611, https://doi.org/10.1039/C8RA01995A.

[28] T. Olmez-Hanci, I. Arslan-Alaton, B. Genc, Bisphenol A treatment by the hot persulfate process: oxidation products and acute toxicity, J. Hazard Mater. 263 (2013) 283–290, https://doi.org/10.1016/J.JHAZMAT.2013.01.032.

[29] N. Potakis, Z. Frontistis, M. Antonopoulou, I. Konstantinou, D. Mantzavinos, Oxidation of bisphenol A in water by heat-activated persulfate, J. Environ. Manag. 195 (2017) 125–132, https://doi.org/10.1016/J.JENVMAN.2016.05.045.

[30] C.M. Dominguez, A. Checa-Fernandez, A. Romero, A. Santos, Degradation of HCHs by thermally activated persulfate in soil system: effect of temperature and oxidant concentration, J. Environ. Chem. Eng. 9 (2021), 105668, https://doi.org/10.1016/j.jece.2021.105668.

[31] C.M. Dominguez, A. Romero, D. Lorenzo, A. Santos, Thermally activated persulfate for the chemical oxidation of chlorinated organic compounds in groundwater, J. Environ. Manag. 261 (2020), 110240, https://doi.org/10.1016/j.jenvman.2020.110240.

[32] Y. Sun, J. Zhao, B.T. Zhang, J. Li, Y. Shi, Y. Zhang, Oxidative degradation of chloroxylenol in aqueous solution by thermally activated persulfate: kinetics, mechanisms and toxicities, Chem. Eng. J. 368 (2019) 553–563, https://doi.org/10.1016/j.cej.2019.02.208.

[33] P. Dobosy, C.É. Vizsolyi, I. Varga, J. Varga, G. Láng, G. Záray, Comparative study of ferrate and thermally activated persulfate treatments for removal of mono- and dichlorobenzenes from groundwater, Microchem. J. 136 (2018) 61–66, https://doi.org/10.1016/J.MICROC.2016.10.015.

[34] M. Gągol, A. Przyjazny, G. Boczkaj, Wastewater treatment by means of advanced oxidation processes based on cavitation – a review, Chem. Eng. J. 338 (2018) 599–627, https://doi.org/10.1016/j.cej.2018.01.049.

[35] K. Fedorov, K. Dinesh, X. Sun, R. Darvishi Cheshmeh Soltani, Z. Wang, S. Sonawane, G. Boczkaj, Synergistic effects of hybrid advanced oxidation processes (AOPs) based on hydrodynamic cavitation phenomenon – a review, Chem. Eng. J. 432 (2022), 134191, https://doi.org/10.1016/J.CEJ.2021.134191.

[36] Q. Xu, H. Zhang, H. Leng, H. You, Y. Jia, S. Wang, Ultrasonic role to activate persulfate/chlorite with foamed zero-valent-iron: sonochemical applications and induced mechanisms, Ultrason. Sonochem. 78 (2021), 105750, https://doi.org/10.1016/J.ULTSONCH.2021.105750.

[37] K. Roy, V.S. Moholkar, Mechanistic analysis of carbamazepine degradation in hybrid advanced oxidation process of hydrodynamic cavitation/UV/persulfate in the presence of ZnO/ZnFe2O4, Separ. Purif. Technol. 270 (2021), 118764, https://doi.org/10.1016/J.SEPPUR.2021.118764.

[38] T. Zhang, Y. Yang, X. Li, H. Yu, N. Wang, H. Li, P. Du, Y. Jiang, X. Fan, Z. Zhou, Degradation of sulfamethazine by persulfate activated with nanosized zero-valent copper in combination with ultrasonic irradiation, Separ. Purif. Technol. 239 (2020), 116537, https://doi.org/10.1016/J.SEPPUR.2020.116537.

[39] K. Fedorov, M. Plata-Gryl, J.A. Khan, G. Boczkaj, Ultrasound-assisted heterogeneous activation of persulfate and peroxymonosulfate by asphaltenes for the degradation of BTEX in water, J. Hazard Mater. 397 (2020), 122804, https://doi.org/10.1016/j.jhazmat.2020.122804.
[40] R.D.C. Soltani, Z. Miraftabi, M. Mahmoudi, S. Jorfi, G. Boczkaj, A. Khataee, Stone cutting industry waste-supported zinc oxide nanostructures for ultrasonic assisted decomposition of an anti-inflammatory non-steroidal pharmaceutical compound, Ultrason. Sonochem. 58 (2019), 104669, https://doi.org/10.1016/j.ultsonch.2019.104669.
[41] R.D.C. Soltani, M. Mahmoudi, G. Boczkaj, A. Khataee, Activation of peroxymonosulfate using carbon black nano-spheres/calcium alginate hydrogel matrix for degradation of acetaminophen: Fe3O4 co-immobilization and microbial community response, J. Ind. Eng. Chem. 91 (2020) 240–251, https://doi.org/10.1016/J.JIEC.2020.08.006.
[42] M.A. Beckett, I. Hua, Elucidation of the 1,4-dioxane decomposition pathway at discrete ultrasonic frequencies, Environ. Sci. Technol. 34 (2000) 3944–3953, https://doi.org/10.1021/es000928r.
[43] H.-S. Son, S.-B. Choi, E. Khan, K.-D. Zoh, Removal of 1,4-dioxane from water using sonication: effect of adding oxidants on the degradation kinetics, Water Res. 40 (2006) 692–698, https://doi.org/10.1016/J.WATRES.2005.11.046.
[44] H.-S. Son, K.-D. Zoh, Effects of methanol and carbon tetrachloride on sonolysis of 1,4-dioxane in relation to temperature, Ind. Eng. Chem. Res. 51 (2012) 8939–8944, https://doi.org/10.1021/ie201766h.
[45] B. Li, J. Zhu, Simultaneous degradation of 1,1,1-trichloroethane and solvent stabilizer 1,4-dioxane by a sono-activated persulfate process, Chem. Eng. J. 284 (2016) 750–763, https://doi.org/10.1016/j.cej.2015.08.153.
[46] D. Tian, H. Zhou, H. Zhang, P. Zhou, J. You, G. Yao, Z. Pan, Y. Liu, B. Lai, Heterogeneous photocatalyst-driven persulfate activation process under visible light irradiation: from basic catalyst design principles to novel enhancement strategies, Chem. Eng. J. 428 (2022), 131166, https://doi.org/10.1016/J.CEJ.2021.131166.
[47] J. Khatri, P.V. Nidheesh, T.S. Anantha Singh, M. Suresh Kumar, Advanced oxidation processes based on zero-valent aluminium for treating textile wastewater, Chem. Eng. J. 348 (2018) 67–73, https://doi.org/10.1016/J.CEJ.2018.04.074.
[48] S. Naim, A. Ghauch, Ranitidine abatement in chemically activated persulfate systems: assessment of industrial iron waste for sustainable applications, Chem. Eng. J. 288 (2016) 276–288, https://doi.org/10.1016/J.CEJ.2015.11.101.
[49] S. Adil, B. Maryam, E.J. Kim, N. Dulova, Individual and simultaneous degradation of sulfamethoxazole and trimethoprim by ozone, ozone/hydrogen peroxide and ozone/persulfate processes: a comparative study, Environ. Res. 189 (2020), 109889, https://doi.org/10.1016/J.ENVRES.2020.109889.
[50] G. Boczkaj, P. Makoś, A. Przyjazny, Application of dispersive liquid–liquid microextraction and gas chromatography with mass spectrometry for the determination of oxygenated volatile organic compounds in effluents from the production of petroleum bitumen, J. Separ. Sci. (2016), https://doi.org/10.1002/jssc.201501355.
[51] P. Makoś, A. Fernandes, G. Boczkaj, Method for the simultaneous determination of monoaromatic and polycyclic aromatic hydrocarbons in industrial effluents using dispersive liquid–liquid microextraction with gas chromatography–mass spectrometry, J. Separ. Sci. 41 (2018) 2360–2367, https://doi.org/10.1002/jssc.201701464.
[52] L. Peng, L. Wang, X. Hu, P. Wu, X. Wang, C. Huang, X. Wang, D. Deng, Ultrasound assisted, thermally activated persulfate oxidation of coal tar DNAPLs, J. Hazard Mater. 318 (2016) 497–506, https://doi.org/10.1016/J.JHAZMAT.2016.07.014.
[53] S. Wacławek, H.V. Lutze, K. Grübel, V.V.T. Padil, M. Černík, D.D. Dionysiou, Chemistry of persulfates in water and wastewater treatment: a review, Chem. Eng. J. (2017), https://doi.org/10.1016/j.cej.2017.07.132.
[54] S. Wang, N. Zhou, Removal of carbamazepine from aqueous solution using sono-activated persulfate process, Ultrason. Sonochem. 29 (2016) 156–162, https://doi.org/10.1016/J.ULTSONCH.2015.09.008.
[55] O.S. Arvaniti, F. Bairamis, I. Konstantinou, D. Mantzavinos, Z. Frontistis, Degradation of antihypertensive drug valsartan in water matrices by heat and heat/ultrasound activated persulfate: kinetics, synergy effect and transformation products, Chem. Eng. J. Adv. 4 (2020), 100062, https://doi.org/10.1016/J.CEJA.2020.100062.
[56] X. Zhao, Z. Cai, T. Wang, S.E. O'Reilly, W. Liu, D. Zhao, A new type of cobalt-deposited titanate nanotubes for enhanced photocatalytic degradation of phenanthrene, Appl. Catal. B Environ. 187 (2016) 134–143, https://doi.org/10.1016/J.APCATB.2016.01.010.
[57] Z. Xu, K. Mochida, T. Naito, K. Yasuda, Effects of operational conditions on 1,4-dioxane degradation by combined use of ultrasound and ozone microbubbles, Jpn. J. Appl. Phys. 51 (2012), 07GD08, https://doi.org/10.1143/jjap.51.07gd08.
[58] Z. Jiang, L. Bingzhi, Degradation kinetic and remediation effectiveness of 1,4-dioxane-contaminated groundwater by a sono-activated persulfate process, J. Environ. Eng. 144 (2018), 4018098, https://doi.org/10.1061/(ASCE)EE.1943-7870.0001445.
[59] G.V. Buxton, C.L. Greenstock, W.P. Helman, A.B. Ross, Critical Review of rate constants for reactions of hydrated electrons, hydrogen atoms and hydroxyl radicals (·OH/·O $^-$ in Aqueous Solution, J. Phys. Chem. Ref. Data 17 (1988) 513–886, https://doi.org/10.1063/1.555805.
[60] C.L. Clifton, R.E. Huie, Rate constants for hydrogen abstraction reactions of the sulfate radical, SO4−. Alcohols, Int. J. Chem. Kinet. 21 (1989) 677–687, https://doi.org/10.1002/kin.550210807.
[61] M.I. Stefan, J.R. Bolton, Mechanism of the degradation of 1,4-dioxane in dilute aqueous solution using the UV/hydrogen peroxide process, Environ. Sci. Technol. 32 (1998) 1588–1595, https://doi.org/10.1021/es970633m.
[62] D. Ouyang, Y. Chen, J. Yan, L. Qian, L. Han, M. Chen, Activation mechanism of peroxymonosulfate by biochar for catalytic degradation of 1,4-dioxane: important role of biochar defect structures, Chem. Eng. J. 370 (2019) 614–624, https://doi.org/10.1016/J.CEJ.2019.03.235.